L-Type Calcium Channel Recording

Uta C. Hoppe, Mathias C. Brandt, Guido Michels and Michael Lindner

Introduction

Calcium channels constitute a large family of voltage- and ligand-operated ion-channels. They share several structural similarities with voltage-gated Na^+- and K^+-channels. All three channel populations appear to originate from the same gene superfamily. Ca^{2+} channels are ubiquitous, they can be found in almost any type of excitable and most unexcitable cells in a wide variety of species.

Their key functional role is to transduce membrane depolarization to an entry of Ca^{2+}-ions into the cell. This important physiological trigger serves as a uniform effector of a vast number of functions in different cells. The specific physiological consequence of Ca^{2+} entry into the cytoplasm depends on the corresponding cell type. An increase in $[Ca^{2+}]_i$ initiates transmitter secretion in nerve terminals and intracellular Ca^{2+} release and sarcomere shortening in skeletal and cardiac myocytes, generates the action potential in cardiac pacemaker cells and regulates gene expression in neurons. When considering the regulation of these processes, it is important to remember the voltage-dependence of most types of Ca^{2+} channels. Due to the voltage-dependence of Ca^{2+} entry, these functionally related and primarily Ca^{2+}-dependent processes acquire a secondary voltage-dependence. In this context, Ca^{2+} ions serve as an intracellular second messenger (Hille 2001).

In cardiac myocytes, at least four types of calcium channels have been discovered, the L-type and T-type Ca^{2+} channels coexisting on the cell surface and the ryanodine receptor and IP_3-receptor on intracellular membranes.

Molecular Diversity of Voltage-Gated Calcium Channels

All voltage-gated Ca^{2+} channels characterized at the molecular level up to now show a similar subunit composition, illustrated in Fig. 1. They consist of five specific subunits: α_1, α_2, linked to δ *via* disulfide bindings, β, located intracellularly, and γ (Hoffmann et al. 1999). The skeletal muscle calcium channel was the first to be characterized at the molecular level. The subunit composition of calcium channel complexes from other tissue types do not exactly resemble those from skeletal muscle.

High threshold Ca^{2+}-channels (HVA, high voltage-activated, non-L-type and L-type channels) activate at more positive membrane potentials, whereas low-voltage activated channels (LVA or T-type, transient, tiny current) require relatively low mem-

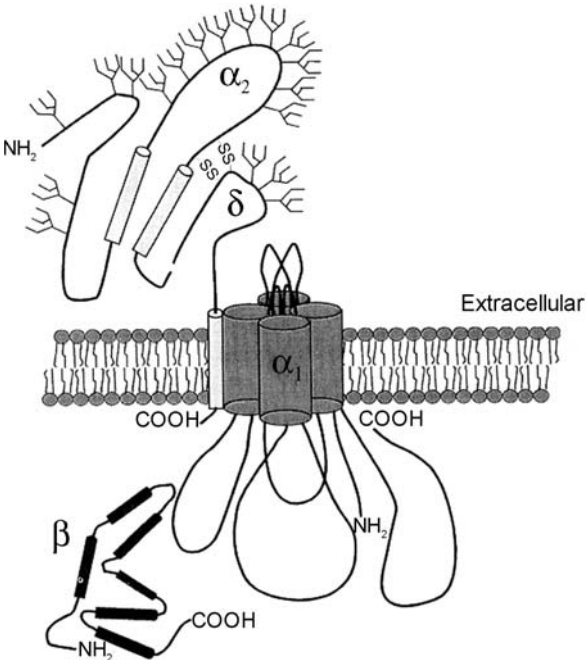

Figure 1
Overview and subunit composition of voltage-gated Ca^{2+} channels. The main structural components are the pore-forming α_1-subunit, accessory α_2 subunit, closely linked to the α_1-subunit *via* the δ-subunit, and the intracellular β-subunit (adapted from Gurnett et al. 1996)

brane potentials for activation. (Fig. 2, Ertel et al. 2000). LVA Ca^{2+} channels comprise $Ca_v3.1$–$Ca_v3.3$ (α_1G, α_1H, α_1I). L-type (long lasting channels) or DHP-sensitive channels are subdivided into four classes according to their α_1-subunit, $Ca_v1.1$ (a_1S, skeletal muscle), $Ca_v1.2$ (α_1C), $Ca_v1.3$ (α_1D, neuronal, pancreas, kidney, endocrine cells) and $Ca_v1.4$ (α_1F, retina). The $Ca_v1.2$ (α_1C)-subunit has several splice-variants, $Ca_v1.2a$ in heart, $Ca_v1.2b$ in smooth muscle and lung and $Ca_v1.2c$ in neurons and heart. Non-L-type or DHP-insensitive channels are encoded by $Ca_v2.1$–$Ca_v2.3$, corresponding to α_1A or P (Purkinje-cell)/Q-type, α_1B or N (neuron)-type and α_1 E or R-type. Distinct recordings of HVA and LVA channels were first made in canine atrial cardiomyocytes (Bean et al. 1985) and guinea pig ventricular myocytes. The estimated density of functional L-type Ca^{2+} channels (1–5/μm^2) is about 10–20 times greater than that of T-type channels.

The pore-forming α_1-subunit (175–275 kD, Fig. 3) is the largest component and determines the characteristic functional and pharmacological properties of every Ca^{2+} channel. It contains the voltage-sensor, the ion-conducting pore, the selectivity filter, binding sites for channel blockers and interaction sites for other subunits. The core α_1-subunit is divided into four homologous repeats or domains (DI-DIV), each consisting of six predicted membrane-spanning segments, S1 to S6, and two short segments, SS1 and SS2, located between S5 and S6. The channel pore is formed by a conformation of S1 to S4, where the linker-connection between the segments S5 and S6, the P(pore)-region, is directed to the inner side of the channel in each of the four repeats. The P-regions from each of the four repeats contain a short SS2 segment with glutamic acid residues of high negative charge density directed to the inner side of the pore, which determine the basis of ion selectivity. Mutations in the amino-acid se-

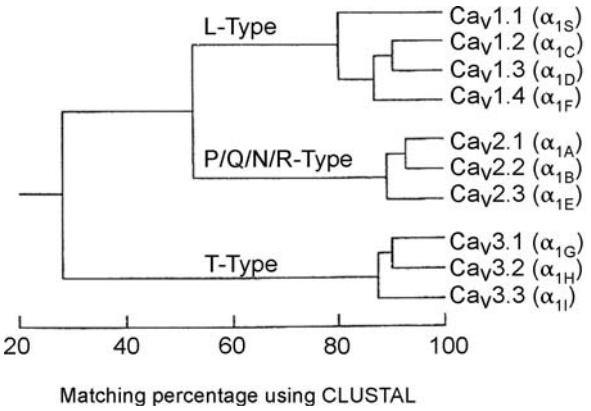

Figure 2
Phylogenetic relationship of voltage gated Ca^{2+} channel subunits illustrated by sequence identities within the membrane-spanning domains of the α_1-subunit. Three large families of Ca^{2+} channels with 80% intra-family sequence identities can be distinguished: L-type channels ($Ca_v1.1$ to $Ca_v1.4$), non-L-type, comprising P/Q,N and R-Type ($Ca_v2.1$ to $Ca_v2.3$) and T-type ($Ca_v3.1$ to $Ca_v3.3$). The corresponding nomenclature of α_1-subunit isoforms is indicated in brackets. (Adapted from Ertel et al. 2000)

quence of this selectivity filter to neutral or positive charges cause alterations in the Ca^{2+} channel affinity for Ca^{2+}, in single-channel conductance and in sensitivity to block by divalent cations. The binding site for pharmacological channel blockers is also located within the P-region of the α_1-subunit. The extracellular mouth of the pore is lined by SS1 and SS2 segments.

The S4-segment contains the voltage-sensor. Like other voltage-gated ion channels, every third residue within the S4-segment of the Ca^{2+} channel contains positively charged domains of arginine or lysine. Depolarization causes a translocation of the S4-segment with positive charge movements across the cell membrane (gating currents), leading to a conformational change in the channel protein from the closed to the open state. Mutations within repeats I and III of the S4 sequence to neutral or negative residues lead to a reduction of gating charge and a reduced sensitivity to membrane depolarization.

While the α_1-subunit alone is sufficient for the expression of functional Ca channels, the other subunits have important regulatory functions for activation, inactivation, gating, and opening probability of the channel pore.

The β-subunit (50–70 kD) is entirely located intracellularly and has several potential phosphorylation sites for cAMP-dependent protein kinases, phosphokinase-C (PKC), and cGMP-dependent kinases. The subunits are not glycosylated and do not co-purify with membranes. β-subunits modulate several parameters of α_1 activity, including the level of channel expression, threshold of activation, rate of inactivation, and steady-state inactivation (Walker and De Waard 1998). The molecular diversity of the β-subunit is caused not only by the expression of four different genes, but also by differential splicing. Four different isoforms, β_1 to β_4, have been identified and are expressed, like the α_2-subunit, in a tissue-specific pattern. β_{1a} is expressed in skeletal muscle, β_{1b} in the brain and β_2 predominantly in cardiac tissue and, to a lesser extent, in aorta, trachea, lung and brain (Biel et al. 1990). The β_3 and β_4 variants are also present in different regions of the brain. Except for the brain β_2-subunit of the rat, the

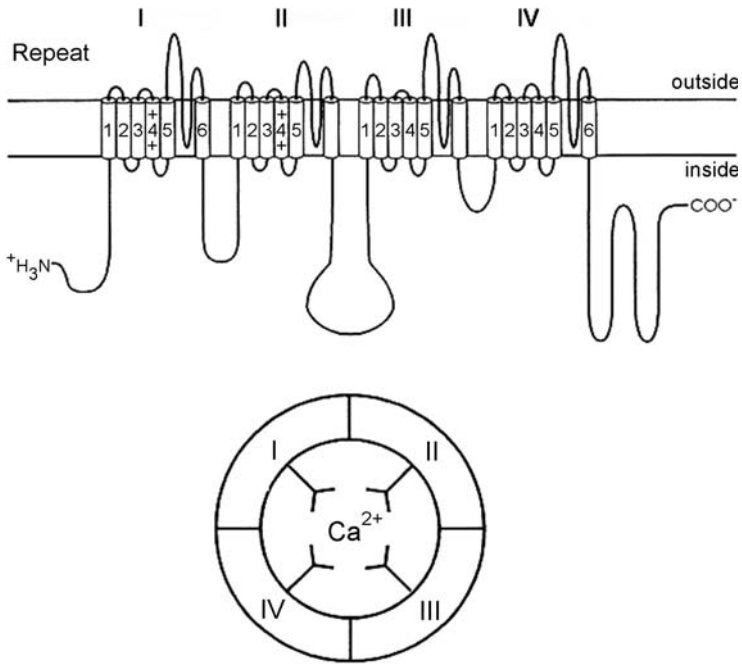

Figure 3
Schematic representation of the α_1-subunit of voltage-gated Ca^{2+} channels. The a_1-subunit consists of four homologous domains, DI to DIV, each consisting of six predicted transmembrane segments, S1 to S6. As illustrated in the inset, a conformation of S1 to S4 in each domain forms the channel pore, with the linker connections between S5 and S6 of domains DI to DIV directed to the inner side of the channel, to form the selectivity filter. (Adapted from Melzer et al., Biochem Biophys Acta 1995; 1241: 59–116)

co-expression of β-subunits with different α_1-subunits facilitates channel pore opening, and results in an increase in the peak-current amplitude. The interaction between α_1 and β-subunits is governed primarily by highly conserved domains in each subunit (α_1- and β-subunit interaction domains; Walker and De Waard 1998).

The disulfide-linked α_2-δ subunit (143 kD and 27 kD) of the voltage-operated calcium channel was the first isolated as a co-precipitate of immunoprecipitated rabbit skeletal muscle DHP receptors. cDNA cloning subsequently revealed that the two subunits are the product of a single gene, being translated from one mRNA and then processed into two proteins of 935 amino acids (α_2-subunit) and 144 amino acids (δ-subunit; Hoffmann et al. 1999). Hydropathy analyses suggest that the δ-subunit has one transmembrane spanning segment with an intracellular C- and an extracellular N-terminus. The α_2-subunit is anchored to the α_1-subunit by this transmembrane domain of the δ-subunit. Different splice variants of the $\alpha_2\delta$-complex with tissue specific expression have been identified. $\alpha_2\delta$-1 is found ubiquitously, $\alpha_2\delta$-2 is expressed in heart, intestinal organs, skeletal muscle and brain and $\alpha_2\delta$-3 is primarily expressed in different parts of the brain (Klugbauer et al. 1999). From electrophysiological studies in different cell types, it can be deduced that co-expression of $\alpha_2\delta$-with α_1- and

β-subunits results in a shift of the current-voltage curve to more positive potentials, an increase in the maximal channel conductance and acceleration of activation and inactivation in α_{1C}- (Bangalore et al. 1996) and α_1 E-type (Quin et al. 1998) calcium channels. This effect appears to be mediated by interaction with the α_{1C}-subunit.

The γ-subunit (25–35 kD) consists of four transmembrane domains and contains two extracellular loops with potential glycosylation sites. Up to now, four tissue-specific isoforms, γ_1 to γ_4 have been identified. The γ_1-subunit is found in skeletal muscle only ($Ca_v1.1{\times}\beta{\times}\alpha_2\delta{\times}\gamma_1$; Eberst et al. 1997), the neuronal γ_2-(stargazin), γ_3-and γ_4-subunits in the central nervous system and the γ_5-subunit in liver, kidney, heart and lung (Klugbauer et al. 1999, 2000). Furthermore, results from Klugbauer et al. (2000) suggest that γ_2-, γ_3-and γ_4-subunits can associate with α_1A, α_1B and α_1 E channels. The γ_5-subunit could be an auxiliary subunit of T-type channels. In rat cardiomyocytes, coexpression of the γ-subunit with the cardiac calcium channel complex leads to a shift in the inactivation curve to more negative potentials and accelerated inactivation, without affecting other voltage-dependent channel properties. Similar results were obtained from co-expression of the γ-subunit with α_1-, β-, and $\alpha_2\delta$-subunits in oocytes.

Biophysical Properties

The basic electrophysiological properties of voltage-dependent L-type calcium channels ($Ca_v1.1$–$Ca_v1.4$) can be characterized by their ion conductance and voltage dependence of activation and inactivation. Important biophysical characteristics are the steep voltage-dependence of activation and inactivation, slow inactivation kinetics and high values for slope conductance. Ca^{2+}-channels activate at membrane potentials around -30 mV and reach their peak whole-cell current amplitude at +10 mV. With further depolarization $I_{Ca.L}$ decreases again, due to a reduction in the electrochemical driving force.

Conductance and Calcium-Permeation

Calcium flow through single L-type Ca^{2+} channels occurs at a rate of ~10^6 ions/s, with an error rate of about ~1 ion in 10^4. Under physiological conditions, calcium channels transport calcium ions and monovalent cations with high selectivity. Even in the presence of other cations, Ca^{2+} is transported almost exclusively.

The kinetics of ion channel transport through the calcium channels differs from free diffusion, even when following the electrochemical gradient. The size of the inward Ca^{2+} current does not increase linearly with $[Ca^{2+}]_o$, but shows the shape of a saturation function. This effect is due to the fact that the permeating Ca^{2+} ions do not pass independently, but compete for the same binding site. Similar results were established for other cations (see Examples).

A major distinguishing feature that has favoured multi-ion occupancy in calcium-channels is the anomalous mole fraction effect (AMFE) between calcium and barium. In the presence of a solution containing equimolar concentrations of Ca^{2+} and Ba^{2+}, the overall channel conductance is smaller than in pure solutions containing either

ion. The AMFE was not found in cardiac L-type calcium channels at single channel level (Yue und Marban 1990), and the validity of the AMFE as an indicator of multiple occupancy has been severely questioned by other authors. Kuo and Hess (1993) proposed that the calcium channel was a multi-ion pore ('two or more site model') that contains two sets of binding sites, one composed of high-affinity sites and located near the external pore mouth, and another composed of low-affinity sites and placed intracellularly.

Kinetics of L-type Calcium Channels

The activation of voltage-dependent ion channels is the result of multiple conformational changes involving positively charged, transmembrane polypeptide regions. Displacement of these charge-bearing intramolecular domains, in response to changes in the transmembrane electric field, produces gating currents. Gating currents, generated by the movement of the channel voltage sensors, are considered to be the primary events in signal transduction for all cellular processes involving voltage-dependent ion channels.

Calcium currents are rapidly activated by depolarisation, reaching a peak in ~2–7 ms, depending on temperature and membrane-potential (E_m). Calcium channel activation appears to depend primarily on E_m, but, as for most voltage-sensitive ion channels, is also sensitive to changes in surface potential. The magnitude of the current across the membrane depends on the density of channels, the conductance of the open channel, and how often the channel is in its open position or its open probability. A possible mechanism is that a change in the membrane potential results in a reorientation of dipoles or an actual charge movement within the membrane field that produces a conformational change in the channel molecule, which in turn results in favouring the open or closed state of the pore.

Activation

Domain I of the ion-conducting α_1-subunit is responsible for calcium channel activation and inactivation (Zhang et al. 1994). The amino acid composition of the S3 and S4 segments within domain I and within the linker connecting between S3 and S4 is critical for the difference in activation kinetics between cardiac and skeletal muscle L-type calcium channels. Activation kinetics, however, are not determined by the IS3 segment and the IS3-IS4 linker alone. The rate of activation is also affected by the current density. On membrane depolarisation, a stretch of S4 moves outward and initiates a number of conformational changes leading to channel opening. The voltage-activated channels seem to open by movement of the inner parts of the S6 α-helices. Conserved proline residues are in the middle of the S4-voltage-sensor of domains I and III in voltage-dependent calcium channels.

As the presence of proline introduces a kink into a helical protein structure, these residues might have an intrinsic function within the voltage sensor ('intrinsic channel agonist'). Yamaguchi et al. (1999) reported that the removal of S4 prolines resulted in a dramatic shortening of channel open time whereas the introduction of extra prolines to the corresponding positions in motif IIS4 and IVS4 increased channel open-time.

Inactivation

L-type calcium channels display calcium-sensitive inactivation, a biological feedback mechanism in which elevation of intracellular calcium concentration speeds up channel inactivation. During sustained depolarisation, voltage-gated calcium channels progressively undergo a transition to a non-conducting, inactivated state, preventing calcium overload of the intracellular space. This transition is triggered by the entry of calcium (calcium-dependent inactivation) and by the membrane potential (voltage-dependent inactivation). Inactivation of L-type calcium channels occurs in two phases, an initial fast phase that depends on a calcium-calmodulin complex binding to the cytoplasmic side of the channel protein and a slower second phase that is voltage-dependent. Both mechanisms act to induce a conformational change in the channel protein, resulting in pore closure.

Calcium-dependent inactivation is only recorded in L-type calcium-channels and is an important regulatory factor for calcium-activated intracellular processes such as excitation-contraction coupling, secretion and gene expression. Calcium ions entering the cell through calcium channels can bind to a specific site located close to the inner mouth of the channel and promote its inactivation. This type of inactivation, as opposed to voltage-dependent inactivation, is not recorded when Ba^{2+} or Sr^{2+} are used as charge carriers (Findlay 2002; see Examples, Fig. 4). Ba^{2+} ions permeate calcium channels even better than Ca^{2+} without producing inactivation.

While voltage-dependent inactivation has been found in all types of calcium channels, the calcium-dependent inactivation seems to be specific for DHP-sensitive L-type calcium channels and has been suggested to arise from a completely different mechanism. The influence of the auxiliary β-subunit on the calcium-dependent inactivation has been tested and it has been suggested that the same molecular determinants affect both voltage- and calcium-dependent inactivation. Up to now, calcium-dependent inactivation of the L-type calcium channel has been considered to be a property of the α_1C-subunit ($Ca_v1.2$), with additional influences from the β- and $\alpha_2\delta$-subunits.

Other types of non-skeletal L-type calcium channels, which are involved in synaptic transmission (P/Q-, R- and N-types), do not show substantial calcium-induced inactivation. Accordingly, different sequences of the α_1C-subunit ($Ca_v1.2$), including a putative EF-hand calcium-binding site, have been shown to be essential for calcium-dependent inactivation (Soldatov et al. 1997). These sequences are located at the carboxy-terminal end of the α_1C-subunit ($Ca_v1.2$) and their transposition to other α_1-subunits transferred calcium-dependent inactivation to channels that do not usually display this type of inactivation. Peterson et al. (1999) showed that calmodulin was necessary for calcium-dependent inactivation and was pre-bound to the C-terminus of the calcium channel. Calcium ions entering as a result of channel opening bound to the tethered calmodulin and led to its interaction with the IQ motif, thereby producing channel inactivation. P/Q-channels have also been shown to be modulated by calmodulin (Lee et al. 1999). The binding mode of calmodulin depends on the free calcium concentration and calcium-binding to calmodulin itself. Other studies suggest that the IQ-motif may not be the only determinant necessary for calcium-dependent inactivation of these channel types.

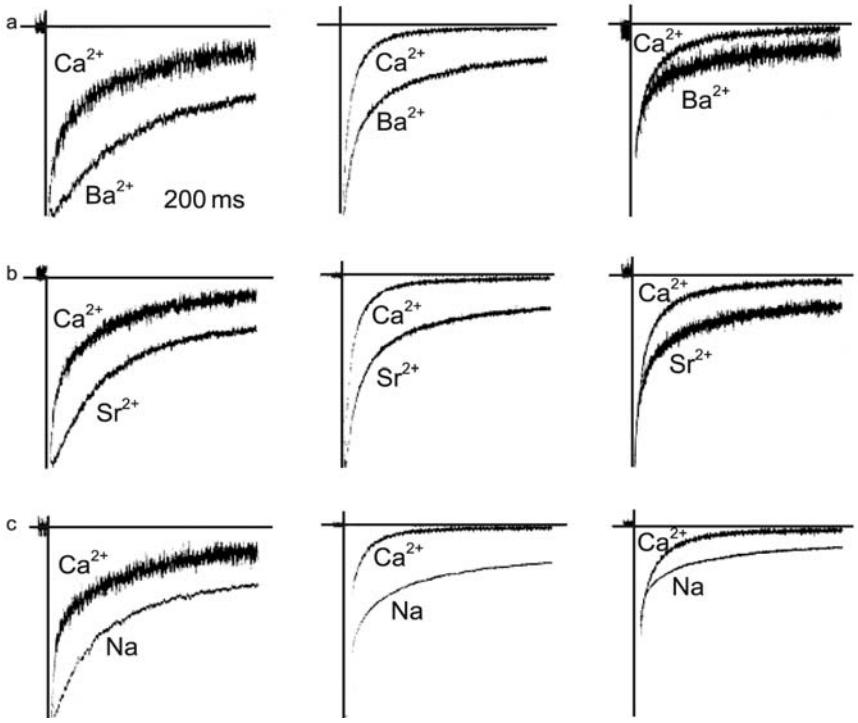

Figure 4
Inactivation kinetics of L-type Ca^{2+} channel current due to different charge carriers. Normalized whole-cell currents elicited by depolarization steps to –20 mV (*left column*), 0 mV (middle column) and +20 mV (*right column*). The superimposed normalized recordings were performed with Ba^{2+} (A), Sr^{2+} (B) and Na^{+} (C) as the main positive charge carrier, compared to recordings with Ca^{2+}. In all three sets of experiments, inactivation was markedly slower when Ca^{2+} was replaced by other ions (Findlay 2002)

L-type Ca^{2+} channels do not inactivate exclusively in a Ca^{2+}-dependent fashion. Voltage-dependent inactivation was distinguished from calcium-dependent inactivation by replacing extracellular calcium with magnesium and recording outward currents through calcium channels.

Inactivation due to voltage has been considered to play a minor role in the decay of L-type calcium current in cardiac myocytes following β-adrenergic stimulation (Findlay 2002). β-adrenergic stimulation slows the voltage-dependent inactivation kinetics of native cardiac L-type calcium channels. The apparent reduction in the voltage-dependent decay of calcium currents induced by isoproterenol (isoprenaline) seems to be due to a conversion of channels from a rapidly inactivating to a slowly inactivating kinetic form. Conversely, Findlay (2002) showed that voltage-dependent inactivation played a major role in the decay of native L-type calcium channels under basal conditions (see Examples). With increasing holding potentials from –20 to +20 mV, a step depolarisation to a fixed pulse potential results in faster inactivation kinetics (Fig. 5). Other investigators (Hirano et al. 1999) showed that strong de-

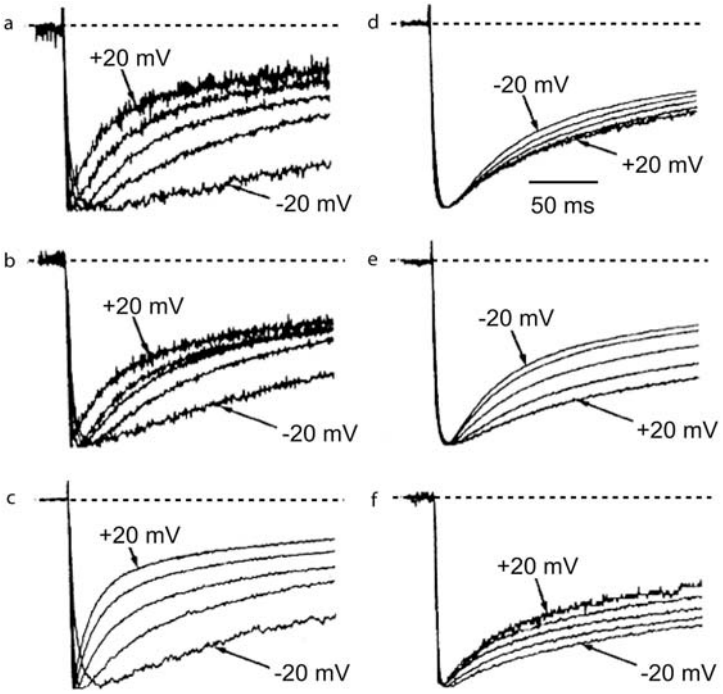

Figure 5
Inactivation kinetics of L-type Ca^{2+} current in relation to different holding potentials and charge carriers. Normalized superimposed whole-cell Ca^{2+} current carried by Ba^{2+} (A), Sr^{2+} (B) and Na^{+} (C) elicited by depolarisation steps to –20 mV, –10 mV, 0 mV, +10 mV and +20 mV. Consistently with all three charge carriers, the channel inactivation was markedly increased with increasing levels of depolarisation, indicating voltage-dependent inactivation. The *right column* (D, E, F) shows the results of the same experiments in the presence of 100 nM isoproterenol (Findlay 2002)

polarisation could evoke 'mode 2' type behaviour in single cardiac L-type calcium channels, this process has also been shown to be enhanced by β-adrenergic stimulation (Yue et al. 1990). It is therefore possible that voltage-dependent potentiation of the L-type calcium current results from the loss of voltage-dependent inactivation. Single amino acids in segments IIIS6 and IVS6 have been identified as determinants of voltage-dependent inactivation. Furthermore, previous studies showed that a segment in IVS5 of the human α_1C ($Ca_v1.2$) subunit is critically involved in inactivation of the channel (Bodi et al. 2002).

Modulation of L-type Calcium Channels

Second messenger-activated protein kinase phosphorylation is a crucial physiological regulative mechanism for the calcium channel protein. cAMP-activated protein kinase A (PKA) increases $I_{Ca(L)}$ whereas the cGMP-activated kinase (PKG) decreases it. Calcium channels can also be regulated directly by G proteins (Gbγ-subunits).

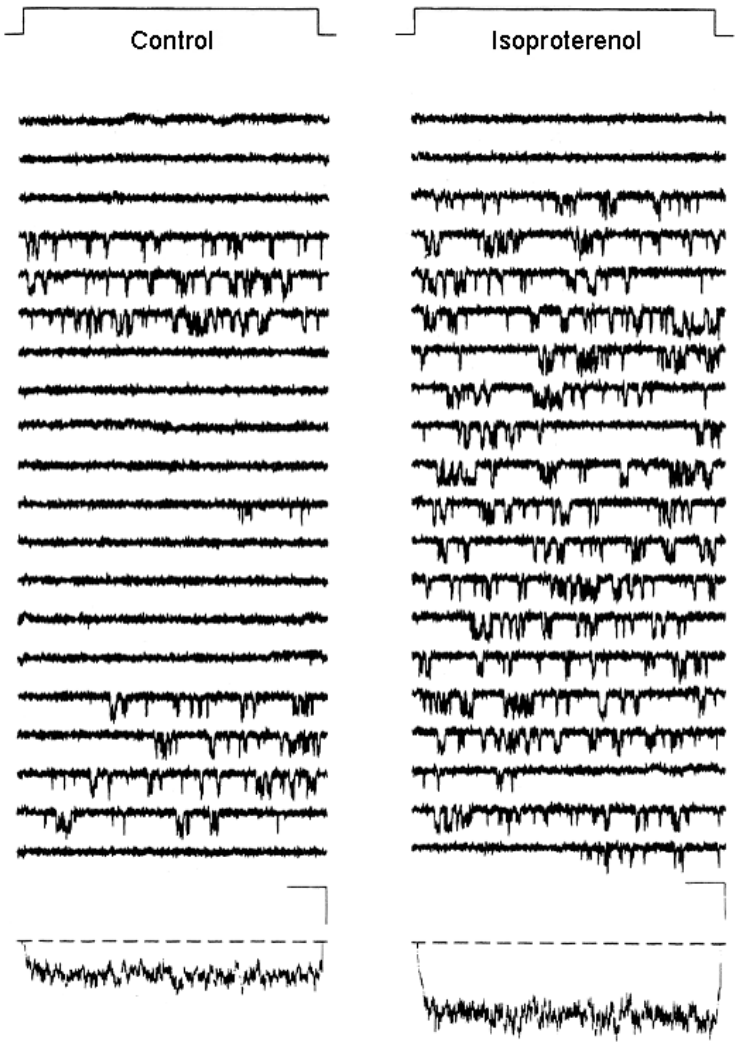

Figure 6
Effect of isoproterenol on Ba^{2+} currents through single L-type Ca^{2+} channels. *Upper part:* Pulse protocol with voltage steps from -100 mV to +20 mV. *Middle:* Unitary current recordings before (*left*) and after (*right*) application of 0.1 mM isoproterenol. *Bottom:* ensemble average current of control (300 sweeps) and isoproterenol (420 sweeps) experiments (Schröder and Herzig 1999)

GTP-binding proteins (G-proteins) exist as heterotrimeric complexes, composed of a Gα-subunit and a Gβγ-dimer. On activation of a G-protein-coupled receptor, the heterotrimer dissociates into free Ga-GTP and Gβγ-dimer. These free Gβγ-subunits are thought to be responsible for fast, membrane-delimited, voltage-dependent G-protein inhibition of certain neuronal voltage-dependent channels. Voltage-dependent modulation of calcium channels by G-proteins causes a decrease in whole-cell current, a depolarizing shift in the current voltage (I–V) relationship and slowed activation kinetics.

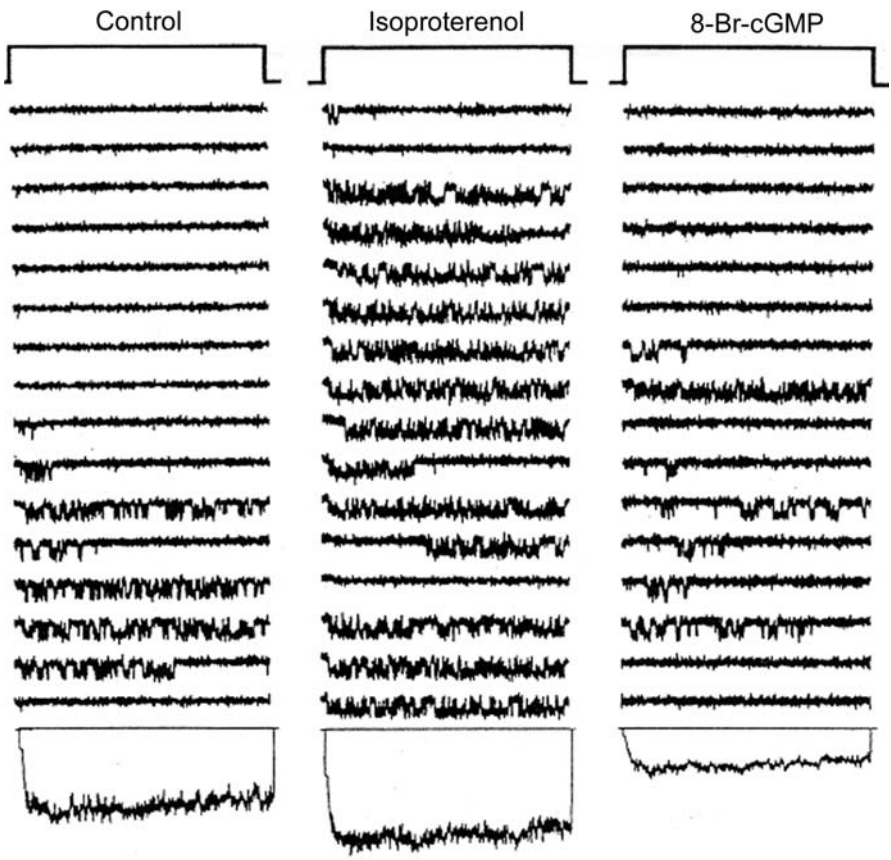

Figure 7
Ba^{2+} currents through single channel L-type Ca^{2+} channels measured in the presence of isoproterenol and 8-Br-cGMP. *Upper part:* Pulse protocol with voltage steps from –100 mV to +20 mV. *Middle:* Unitary current recordings in with added isoproterenol (*left*) and additional 8-Br-cGMP. *Bottom:* ensemble average current of isoproterenol (600 sweeps) and 8-Br-cGMP (600 sweeps) experiments. The scale bars indicate 20 ms (horizontal), 2 pA (unitary current traces) and 50 fA (ensemble average current), respectively (Klein et al. 2000)

Another characteristic is the loss of G-protein modulation with large depolarisations. Consequently, a large depolarizing prepulse immediately preceding a test pulse transiently removes inhibition, and activation is accelerated, a phenomenon referred to as prepulse facilitation (Bean 1989). Native cardiac L-type channels have long been known to exhibit G-protein-induced stimulation *via* the $G\alpha_s$- and cAMP-dependent protein kinase pathway. Viard et al. (1999) demonstrated stimulation of smooth-muscle L-type currents by $G\beta\gamma$ *via* a phosphoinositide 3-kinase pathway. Inhibition *via* activation of $G\alpha_{i/o}$, and subsequent inhibition of adenylate cyclase, is another modulatory G-protein path that regulates cardiac L-type channels.

Several studies have shown that the α_1C-subunit is a substrate for PKA *in vitro*, and Ser1928 has been identified as a potential PKA target. Channel phosphorylation leads to an increase in channel activity. The target protein of PKA is a sub-membrane

protein, called AKAP79 (A-kinase anchoring protein). Mutations of Ser1928 to alanine in the C-terminus of the α_1C-subunit resulted in a complete loss of cAMP-mediated phosphorylation and a loss of channel regulation.

Stimulation of the β-adrenergic receptor with zinterol or isoproterenol has been shown to increase Ca^{2+} single channel currents (Schröder and Herzig 1999; Fig. 6). In mouse ventricular myocytes 8-Br-cGMP reverses all isoproterenol-induced changes in L-type calcium channel gating (Klein et al. 2000; Fig. 7).

Pharmacology

Pharmacological modulation of the L-type Ca^{2+} current and its molecular basis have been the subject of extensive experimental studies in the past decades. Although most Ca^{2+} channel agonists and antagonists are not completely selective for different Ca^{2+} channel subtypes, the application of specific channel blockers has been an extensively used criterion to distinguish between different types of Ca^{2+} channels. The ability of different compounds to block or enhance L-type calcium current depends on substance-specific properties and their ability to interact with particular binding sites on the channel complex.

Binding Sites

Although the auxiliary subunits have important regulatory influences, all essential pharmacological and biophysical properties of L-type Ca^{2+} channels are determined by the α_1-subunit. All major compounds with the ability to alter L-type Ca^{2+} current properties interact here. The high sensitivity of L-type Ca^{2+} channels towards different classes of antagonists is unique among other Ca^{2+} channel isoforms.

The principal chemical classes of Ca^{2+} channel inhibitors are 1,4-dihydropyridines (DHP), phenylalkylamines (PAA) and benzothiazepines (BTZ). From initial experimental studies, it was proposed that distinct binding sites exist in the α_1-subunit of the L-type Ca^{2+} channel for each of the three substance groups. Antagonists from each group are able to affect each others' binding abilities in a non-competitive manner, leading to an "allosteric" model of Ca^{2+} antagonist binding (Fig. 8). Glossmann et al. (1983) showed that verapamil, gallopamil, and the inorganic Ca^{2+} channel antagonist La^{3+} inhibited diltiazem binding non-competitively in a temperature-dependent manner. DHP binding was inhibited by verapamil binding but stimulated by (+)cis-diltiazem. The affinity to isradipine, a DHP compound, was increased by diltiazem at 37 °C, but incompletely inhibited at 2 °C (Glossmann et al. 1983). Other investigators confirmed a temperature-dependent potentiation of diltiazem Ca^{2+} channel block in hamster cardiomyocytes by nitrendipine, which in itself did not have a blocking effect. PAAs competitively inhibited BTZ binding in rabbit skeletal muscle with a slope factor of about 1.

These and other observations of a direct antagonism between PAA and BTZ binding have led to the assumption that the binding domains of the two calcium antagonists are identical. However, PAA binding increases the dissociation rate of BTZ from the Ca^{2+} channel, which is not the case between different BTZ compounds (Hagiwara

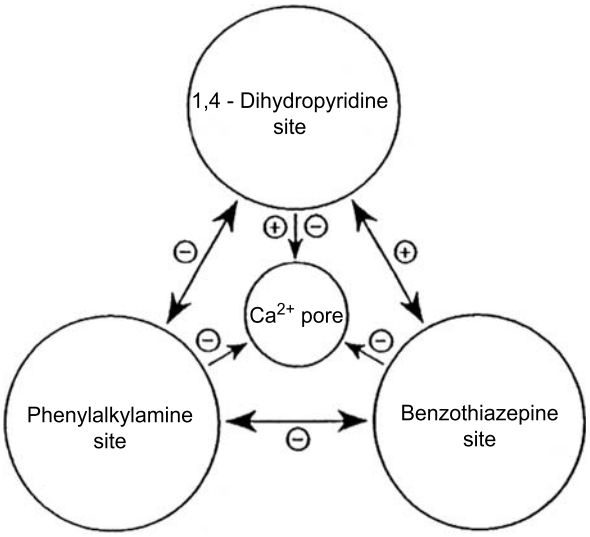

Figure 8
Allosteric model of Ca^{2+} antagonist interaction sites on the α_1-subunit of L-type Ca^{2+} channels. Dihydropyridines (DHP), phenylalkylamines (PAA) and benzothiazepines (BTZ) influence each others' binding properties to the α_1-subunit. This has been attributed to allosteric interaction between the three closely related binding sites. (Adapted from Triggle, J Cardiovasc Pharmacol 1996; 27 (Suppl A): S11–S16)

et al. 1997). In contrast to the allosteric model, Mitterdorfer et al. (1998) propose an "amphiphilic multisubsite domain" with the assumption of a single pore-associated site, accommodating different chemical classes of drugs.

The three major classes of Ca^{2+} antagonists bind to the channel α_1-subunit in close proximity to each other near the channel pore and close to the Ca^{2+} binding site. The domains III and IV in S6 and III in S5 form a pocket that serves as a "hot spot" for drug binding and drug action.

More precise structural information on the binding site for DHP and other Ca^{2+} antagonists was obtained from photoaffinity labelling studies using photoreactive DHP and PAA molecules. Glossmann et al. (1987) incorporated 1,4-dihydropyridine (azidopine) and other compounds into purified skeletal L-type Ca^{2+} channels and identified the site of labelling by proteolysis and immunoprecipitation of the α_1-subunit.

With these initial and other experiments, high-affinity Ca^{2+} antagonist-binding determinants were identified within the S6 segments in repeats III and IV and the extracellular portion of linker connection IIIS5-S6. As both segments are located in the centre of the channel molecule, these mapping results suggested that the drug-binding domains were located close to the ion-conducting pathway. Information on specific amino acids required for Ca^{2+} antagonist binding were obtained from various mutational analyses, mostly involving modifications of the α_1-subunit. These included alanine-scanning experiments where individual amino acid residues which differed between L-type and non L-type channels were systematically replaced by alanine. The novel α_1-subunits were expressed in mammalian cells with other subunits to determine their drug-binding properties. Peterson et al. (1997) showed that mutation of four residues in IIIS6 (Tyr-1152, Ile-1153, Ile-1156 and Met-1161) and one in IVS6 (Asn-1472) reduced DHP binding affinity more than five-fold. In a "gain-of-function"

approach, specific photoaffinity-labelled regions of antagonist-sensitive L-type Ca^{2+} channels were transferred to homologous regions of the α_1-subunit in non-L-type channels.

Interaction with Ca^{2+}

The drug-binding properties of Ca^{2+} channels are modulated substantially by the presence of channel-bound Ca^{2+} ions. The great selectivity of calcium channels for Ca^{2+} ions depends on the selectivity filter that contains a highly specific Ca^{2+} binding site. It is constituted of 4 glutamate residues conserved throughout all Ca^{2+} channels located in the pore-forming S5-S6 linker helices. At this site, one Ca^{2+} ion is bound with a K_D of 0.7 μM and blocks the channel pore (non-conducting state). The second Ca^{2+} ion is bound with a K_D of about 100 mM and allows permeation of the previous ion.

In the absence of extracellular Ca^{2+}, the sensitivity of L-type Ca^{2+} channels to Ca^{2+} antagonists is markedly decreased. In a different approach, it could be shown that mutation of the high-affinity Ca^{2+} binding selectivity filter also decreased DHP binding. This indicates that Ca^{2+} ions must occupy a high-affinity Ca^{2+} binding site in order to stabilize high-affinity DHP binding. Peterson and Catterall (1995) considered a possible allosteric mechanism of interaction between Ca^{2+} and the DHP binding site. When the glutamate residues in the S5-S6 domain were replaced by glutamine in a_1C (Mitterdorfer et al. 1995, 1996) or a_1S (Peterson et al. 1995) calcium channels, there was an 11- to 35-fold decrease in the Ca^{2+} binding affinity. The sensitivity to DHPs was also reduced.

Only when a higher extracellular Ca^{2+} concentration was applied, could DHP sensitivity be restored, indicating the importance of Ca^{2+} ions in stabilizing the binding of DHP to its binding site in the channel. Two Ca^{2+} ions bound to the Ca^{2+} channel α_1-subunit, on the other hand, destabilize the binding of all classes of Ca^{2+} antagonists.

Ca^{2+} Channel Agonists and Antagonists

The three 'classic' groups of calcium channel blockers contain derivates of the chemically unrelated dihydropyridines (nifedipine), phenylalkylamines (verapamil) and benzothiazepines (diltiazem), that had originally been developed as coronary vasodilators in the early 1960s.

Even before voltage-clamp experiments were performed, the observation that their inhibitory influence on skeletal muscle contraction force and cardiac contractility could be reduced by increasing the level of extracellular Ca^{2+} led to their definition as 'Ca^{2+} antagonists'. Higher (millimolar) concentrations of divalent cations inhibited drug binding to all domains. Therefore one or more Ca^{2+} binding sites allosterically coupled to the drug-binding domains were included into the allosteric model.

Despite their high affinity to individual binding sites within the a_1-subunit, calcium antagonists do not bind exclusively to L-type calcium channels. All types of calcium antagonists have been reported to bind with lower affinity to various other membrane proteins including T-type Ca^{2+}-channels, Na^+-channels, K^+-channels and membrane transporters.

Dihydropyridines

1,4-Dihydropyridines (DHP) are very selective modulators of L-type Ca^{2+} channels (Ca_v1-family, namely α_1S, α_1C, α_1D, α_1F or $Ca_v1.1$, $Ca_v1.2$, $Ca_v1.3$, $Ca_v1.4$). The different members of this pharmacological group can be divided into Ca^{2+} channel agonists and antagonists. Classic compounds among DHP calcium antagonists are nifedipine, nitrendipine, amlodipine, felodipine and isradipine. The highly lipophilic DHP derivates access the calcium channel protein through the lipid phase of the membrane (lipophilic path). Because of their very poor water solubility, it is unlikely that the drugs enter into the channel from the cytoplasmic side. Therefore, the DHPs appear to bind to the channel at or near the channel/lipid interface behind the P loop. Antagonists showed non-polar interactions with the residues at the crossing of domains III and IV S6 helices at the bottom of the crevice that could prevent helical movements involved in activation by stabilizing the closed state. Agonists in this conformation were not able to interact with the hydrophobic crossing residues and lead to a destabilizing of the closed state (Lipkind and Fozzard 2003).

The preferential effect on different parts of the vascular bed is determined by the chemical structure of the different types of DHP compounds. The first generation DHP, nifedipine, primarily acts on the peripheral vasculature and coronary arteries, reducing the peripheral vascular resistance and thus lowering blood pressure. Amlodipine, felodipine and isradipine are more potent blockers of Ca^{2+} channels in peripheral vascular smooth muscle. Nimodipine acts more selectively in cerebral vascular smooth muscle cells. This remarkable tissue sensitivity is caused by the different blocking properties of these DHP compounds.

Like the other classes of Ca^{2+} antagonists, DHP binding to the α_1-subunit of the L-type Ca^{2+} channel depends on the transmembrane segments IIIS6, IVS6 and the S5-S6 linker in repeats III and IV of the channel protein. Amino acids responsible for DHP or PAA interaction in transmembrane segments IIIS6 and IVS6 were identified by systemic replacement with alanine or non-L-type α_1 (α_1E, α_1B) sequences. Results from photoaffinity labelling studies have shown that further residues in the transmembrane segment IIIS5 are crucial for DHP interaction. In addition to the two IIIS5 residues, at least eleven additional amino acids, seven in IIIS6, participate in the formation of the binding pocket for DHPs. Additional binding sites with specific importance for DHP were identified in repeat I and repeat III of the α_1-subunit. In IIIS5, nine amino acid residues differ between L-type and non-L-type Ca^{2+} channels. A part of the DHP interaction domain already exists in non-L-type calcium channels, but is not sufficient for high-affinity DHP sensitivity. The co-expression of β-subunits dramatically enhanced L-type α_1-subunit-associated high-affinity DHP binding. β-subunit association seems to cause a conformational change in α_1-subunits, similar to the

action of Ca^{2+}, which converts the DHP binding domain to a high-affinity state. This can be summarised as low-affinity (β-subunit deficient) and high-affinity (β-subunit present).

Dihydropyridines exert voltage-, enantioselective- and use-dependent block of L-type calcium channels. The state-dependent interaction (voltage- and use-dependent action) has been demonstrated in terms of the well-accepted modulated-receptor hypothesis. The extent of the DHP block of L-type calcium channels depends on the holding potential and increases with more depolarizing membrane potentials at which the channels start to inactivate. Hydrophobic molecules like nifedipine and nitrendipine preferentially bind to the inactivated state of the calcium channel at depolarized membrane potentials. At holding potentials of -80 mV, where L-type Ca^{2+} channels are in the resting state, DHP block is much weaker. These findings explain why vascular smooth muscle cells (membrane potential about -50 mV) are blocked more effectively by first generation Ca^{2+} antagonists like nifedipine than ventricular cardiomyocytes (membrane potential about -80 mV; Adachi-Akahane 2000).

By construction of chimeric α_1 subunits and pharmacological characterization after coexpression with $\alpha_2\delta$- and β_{1a}-subunits in Xenopus oocytes, Mitterdorfer et al. (1996) identified Thr1066 and Gln1070 as necessary for DHP antagonist (isradipine) and agonist (–)Bay K 8644) actions. While isradipine required only Thr1066, and the presence of Gln1070 only increased the channel sensitivity to the DHP antagonist, DHP agonist modulation by Bay K 8644 depended on the additional presence of Gln1070.

Like other classes of calcium antagonists, the newer DHPs do not bind to L-type Ca^{2+}-channels alone. In rat hippocampal neurones, nicardipine, nifedipine and nimodipine block T-type Ca^{2+}-channels in a use-dependent way. Nicardipine blocks voltage-gated K^+-channels in cerebellar neurons. Like tertiary amine local anaesthetics, nifedipine blocked Na^+ currents in rat ventricular neonatal cardiomyocytes in a dose-dependent fashion; Na^+ current restitution was achieved by additional application of Bay K 8644.

DHP Ca^{2+} Agonists

DPH-derivates like S(–)Bay K 8644, CGP 28–392, (+)S202–791 and YC-170, the benzoylpyrrole FPL 64176 and the benzodiazocine CGP 48506 are known to act as Ca^{2+} channel agonists. They have been developed as scientific tools but are not used therapeutically. The chemical differences between agonist and antagonist 1,4-dihydropyridines lies in their chemical structure – DHP-calcium channel blockers have two freely rotating ester groups whereas the agonists have only one. Agonist activity is produced only by substitution of small polar groups in the ester group on the left side (Lipkind and Fozzard 2003). Bay K 8644 modulates L-type Ca^{2+} channels in two ways: one enantiomer (+)Bay K 8644 acts as a Ca^{2+} antagonist, the stereoisomer (–)Bay K 8644 shows agonistic effects (Adachi-Akahane et al. 2000). In the presence of Bay K 8644, Ca^{2+} influx through the L-type Ca^{2+} channel during depolarization is increased by interaction with the open state of the channel. In contrast to DHP-antagonists, 1,4-dihydropyridine activator interactions are significantly less voltage-dependent.

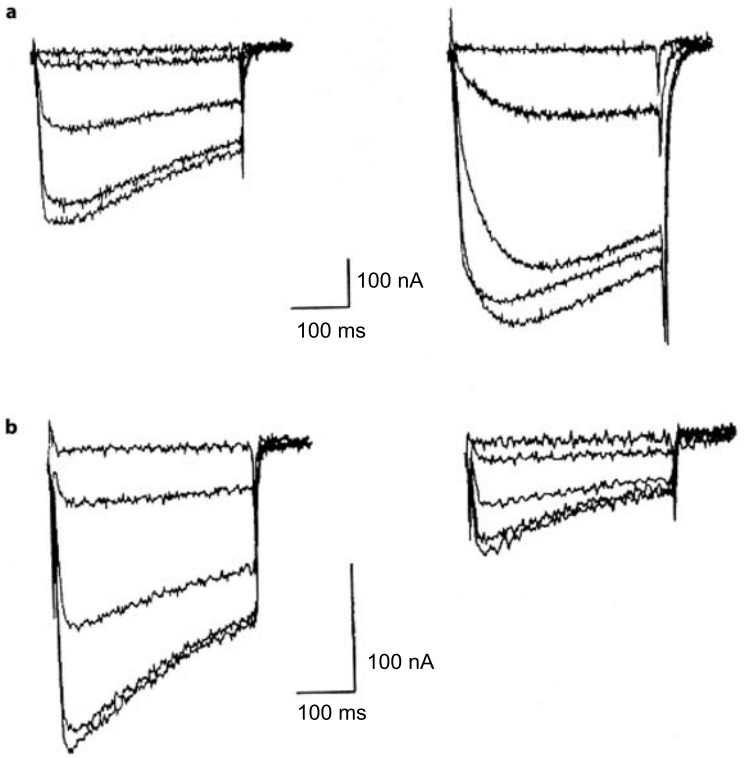

Figure 9a,b
Modulation of Ba^{2+} current through chimeric L-type Ca^{2+} channels by Bay K 8644 (**a**) and isradipine (**b**). Experiments were performed in the presence of 40 mM Ba^{2+} at test potentials from -30 mV to +10 mV (Grabner et al. 1996)

Kokubun et al. (1984) demonstrated this by whole-cell and single-channel studies with Ba^{2+} as charge carrier. The whole-cell current amplitude in neonatal rat cardiomyocytes increased in a concentration-dependent fashion up to 3.5-fold in the presence of 10^{-7} M Bay K, consistent with an increase in the single-channel slope-conductance from 18.3 pS to 24.0 pS. This could be related to an increase in the number of available open channels with long channel openings and a marked prolongation of the channel mean open time in the presence of Bay K 8644. These effects were independent of intracellular cAMP levels, indicating that phosphorylation steps of channel subunits were not involved. Similar effects of BayK with an increase in whole cell current and longer openings in single-channel measurements were obtained by Grabner et al. (1996) and Michels et al. (2002, see Examples). Both DHP compounds bind to a common binding site in the calcium channel protein.

Sanguinetti et al. (1986) reported that the influence of Bay K 8644 on Ca^{2+} channel gating properties in calf Purkinje fibres is not unanimously agonistic but, as for other DHPs, shows voltage-dependent, frequency-dependent and concentration-dependent variations. When hyperpolarizing membrane potentials (-60 mV) were applied as conditioning prepulse, the peak Ca^{2+} current was enhanced, due to a shift of the I-V

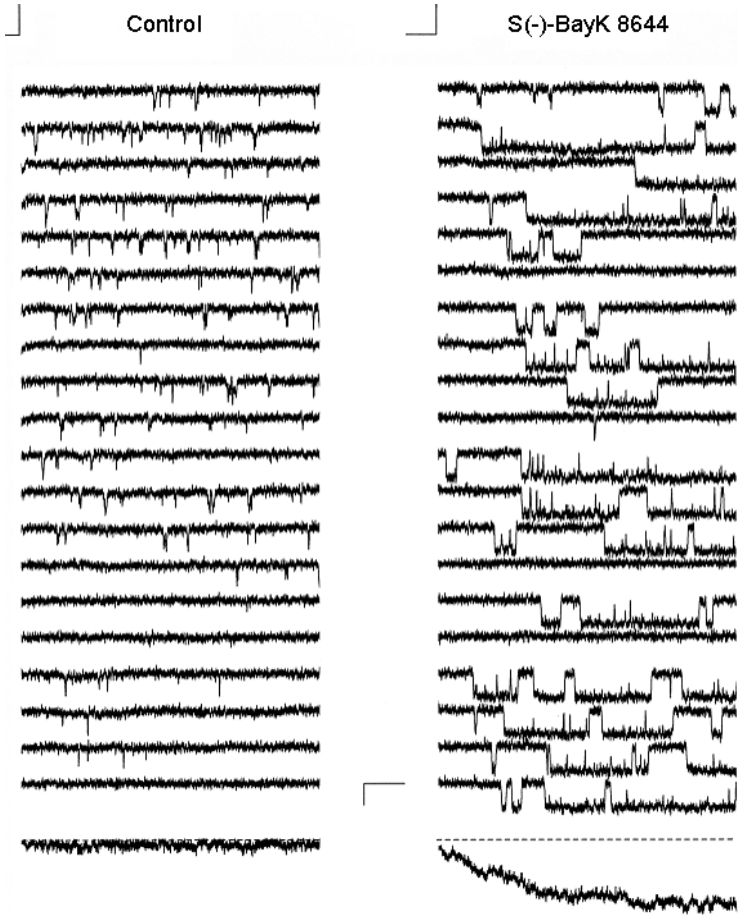

Figure 10
Effect of S (–)Bay K 8644 on L-type $Ca2^{+}$ channels. Upper part: Voltage-protocol at a holding potential of -90 mV and test potential of +10 mV. Middle: original single channel sweeps recorded at a pulse duration of 150 ms. Below: Ensemble average current from 117 sweeps (control) and 179 sweeps (0.1 mM Bay K 8644). The scale angle indicates 15 ms (*horizontal*) and 1 pA (*vertical*) for single channel traces, 0.075 pA for ensemble average current (Michels et al. 2002)

curve in the hyperpolarizing direction and faster rates of inactivation over a wide range of test potentials. At depolarizing prepulses (20 mV) the current amplitude was decreased. The agonistic effect on inward current was also diminished in the presence of high pulse-frequencies. These effects could be attributed to modulation of Ca^{2+} channel gating currents by Bay K 8644, caused by a drug-induced slowing of the transition of the Ca^{2+} channel from the open to the closed channel. The effect of BayK 8644 application on whole-cell Ca^{2+} current through chimeric Ca^{2+} channels is demonstrated in Fig. 9. Single L-type Ca^{2+} channel recordings from human hMT cells in the presence of 0.1 mM BayK 8644 are demonstrated in Fig. 10 (see Examples).

Phenylalkylamines

Beside verapamil, the classic phenylalkylamine (PAA), two other compounds from this group have been extensively studied: methoxyverapamil (D600/gallopamil) and desmethoxyverapamil (D888/devapamil). The only PAA currently in clinical use is verapamil, a potent drug for slowing AV-nodal transmission, which is used in the treatment of supraventricular tachycardias.

As the binding sites for PAAs, DHPs and BTZs are located close to each other, with possible allosteric interaction at the α_1-subunit, PAA binding interferes with channel block by compounds from both other substance groups. The affinity of Ca^{2+} channels for PAAs is higher than those for DHP and BTZs. Within the PAAs, the binding affinity to L-type Ca^{2+} channels is in the order desmethoxyverapamil > methoxyverapamil > verapamil. All PAA compounds have a chiral centre and exist as levorotatory (–) and dextrorotatory (+) enantiomers, where the (–) enantiomers are the more potent calcium antagonists.

Like DHPs, Ca^{2+} channel block by phenylalkylamines is voltage- and state-dependent, as the different conducting states of Ca^{2+} channels, resting, open or inactivated, have different affinities to PAAs. The affinity to PAA block is greatest when a major proportion of the Ca^{2+} channels is in the inactivated, non-conducting state, and lowest at membrane potentials near -70 mV, when the most of the channels are in the resting state. Drug binding and electrophysiological studies indicate that this preference can be explained by a conformational change within the PAA binding site on the α_1-subunit caused by membrane depolarisation. In contrast to dihydropyridines, PAA block of Ca^{2+} channels also shows marked use-dependence. Verapamil and diltiazem have prominent frequency-(use-)dependent antagonisms and nifedipin exhibits prominent voltage-dependent block. This explains the antiarrhythmic and cardiac depressant properties of verapamil and diltiazem and the general vascular selectivity of 1,4-dihydropyridines.

Several authors have shown that rapid trains of depolarisations cause an increased fraction of drug binding to inactivated channels, with progressive reduction of whole cell current. The extent of use-dependent calcium current block increases with higher stimulation frequencies and increasing pulse durations – and differs markedly between different classes of calcium antagonists.

As pointed out by Kanaya et al. (1983), high affinity drug binding to the inactivated state slows the transition of the channel protein to the resting state and thereby stabilizes channel inactivation. Consistently, the time constant of recovery from block at -70 mV is longer for PAAs ($\tau 2 = 2.4$ min; McDonald et al. 1984) compared to DHPs (τ_1=1.5 s, t_2=30 s; Sanguinetti and Kass 1984). This characteristic is of clinical importance for PAA Ca^{2+} antagonists as antiarrhythmics. Frequency-dependent block with prolonged recovery from the inactivated state slows down transmission of excitation at the AV-node and reduces the ventricular rate in supraventricular tachyarrhythmias.

The PAA binding site at the Ca^{2+} channel α_1-subunit has been characterized by similar experimental methods to those used in studies of the DHP binding site, including photoaffinity labelling, alanine scanning experiments and expression of genetic constructs. Amino-acid residues with PAA binding function were identified in

segments IIIS6 and IVS6. The IVS6 residues and Ile1153 from segment IIIS6 are specific for L-type Ca^{2+} channels. These amino acid residues are not present in non-L-type Ca^{2+} channels and may therefore be responsible for their low PAA sensitivity. The two residues (Phe1164 and Val1165), which are very close to the intracellular C-terminal end of IIIS6 and are uninvolved in DHP-binding, showed a ~10-fold decrease in affinity for D888 upon alanine substitution. Individual mutation of any of these residues to alanine or glutamine decreased PAA sensitivity 10- to 60-fold.

Benzothiazepines

The most relevant compound and the only one in clinical use from the group of benzothiazepine (BTZ) calcium antagonists is diltiazem. Other compounds are SQ32,910, which has a higher affinity for L-type Ca^{2+} channels than diltiazem, and (+)cis-azidodiltiazem, which is used for photoaffinity labelling experiments. The properties of BTZs are intermediate between those of DHPs and PAAs in a number of chemical and pharmacological respects. Their potency as peripheral vasodilators is weaker than that of nifedipine or nitrendipine. Compared to verapamil, they have a weaker negative chronotropic effect on the SA- and AV-node, and only a modest negative inotropic effect on the ventricular myocardium. BTZs are moderately selective for L-type Ca^{2+} channels in vascular smooth muscle cells. As for the other groups of calcium antagonists, diltiazem blocks other types of ion channels at higher concentrations (40 μM and above), including N-, R- and P/Q-type Ca^{2+} channels in neurons (Diochot et al. 1995).

All BTZ compounds have two chiral centres and exist in four possible diastereoisomers, where the corresponding (+) isomers are more potent Ca^{2+} channel blockers. As for DHPs and PAAs, BTZ binding alters the binding properties of the other classes of calcium antagonists to their binding sites, showing a temperature-dependent effect. At 25 and 37 °C, nitrendipine binding was enhanced to 140% and 200% of control respectively in the presence of 10 μM diltiazem. At 0 °C however, nitrendipine binding was reduced to 68%, indicating allosteric modulation of the spatially closely related binding sites of BTZs and PAAs.

The properties of BTZ binding to L-type Ca^{2+} channels also indicate an intermediate place between DHPs and PAAs. Diltiazem binding causes more resting block than verapamil but less than nitrendipine. The same applies to the question of frequency dependence. In a train of depolarizations, diltiazem reaches the maximum level of blockade more slowly than nitrendipine, where use-dependent block is virtually absent, but faster than verapamil, which shows marked use-dependence. These findings are consistent with time constants for channel recovery from diltiazem block (τ=2 s) being intermediate between those for nitrendipine (τ=0.5 s) and verapamil (τ=15 s).

Bodi et al. (2002) showed that a segment in IVS5 of the human α_1C ($Ca_v1.2$) subunit is critically involved in inactivation of the channel. Mutants constructed in this region lost the characteristic use-dependent block by PAA and BTZ and recovered from inactivation significantly faster after drug block compared with the wild type Ca^{2+}-channel.

The BTZ binding side of the L-type Ca^{2+}-channel is formed by amino acid residues in segments IIIS6 und IVS6, located in close proximity to the PAA binding site. PAA and BTZ share residues Tyr1463, Ala1467, and Ile1470 in segment IVS6 as common binding motifs.

PAAs and BTZs possess a distinct structure-activity relationship for blocking but access their binding domains from opposite sides (PAAs, the cytoplasmic side, BTZs, the extracellular side) of the channel. To investigate the access of BTZs to their binding site on the α_1-subunit, comparative studies were performed with SQ32,910, a tertiary BTZ, and SQ32,428, its quaternary derivate, which supported the theory that BTZ Ca^{2+}-antagonists access their binding site from the extracellular side of the cell membrane.

Description of Methods and Practical Approach

Recording Techniques

Whole Cell Recording

The study of calcium channel function in whole cell configuration depends to a great extent on the patch clamp method, using single myocytes. Various methods of dissociation of myocardial and non-myocardial myocytes have been published in the past. In whole-cell experiments, a thin pipette with tip resistances, depending on the experimental settings, around 3–5 MΩ is placed at the front of a head stage connected with a patch clamp amplifier and a computer unit to control holding- and test-pulse potentials. The head stage is connected with a syringe used to generate negative pressure at the tip of the patch pipette. The pipette is filled with electrolyte solution equivalent to intracellular ion concentrations.

Electrolyte Solutions

When recording native Ca^{2+} channels in cardiomyocytes, the typical extracellular solution contains about the following [mM]: TEA 126, CsCl 5.4, $CaCl_2$ 2, $MgCl_2$ 1, NaH_2PO_4 0.33, dextrose 10, and HEPES 10. The pH is adjusted to 7.4 with CsOH. The pipette solution replaces the intracellular medium of the cell once the whole-cell configuration is achieved. A typical composition is [mM]: Cs-aspartate 110, CsCl 20, $MgCl_2$ 1, EGTA 10, GTP 0.1, Mg-ATP 5, HEPES 10 and Na_2-phosphocreatinine 5. The pH is adjusted to 7.4 with CsOH. Ca^{2+} ions are replaced by equimolar amounts of Ba^{2+} or other charge carriers if desired.

Pipette Preparation

Patch pipettes with a tip resistance, depending on the experimental settings, around 2–4 MΩ, are pulled from borosilicate glass capillaries, filled with intracellular solution and placed into the head stage for experiments without delay.

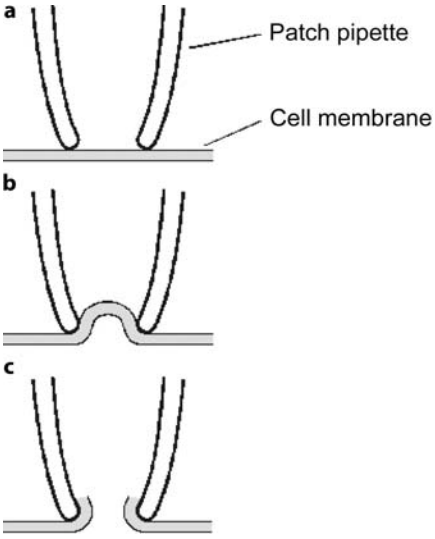

Figure 11a–c
Sequence of pipette configurations during whole-cell patch-clamp experiments: After positioning of the pipette on top of the cell membrane (**a**), gentle vacuum suction is applied to the pipette tip by a syringe attached to the pipette holder to establish a high resistance connection (Giga-ohm seal) between pipette tip and membrane in the cell-attached configuration (**b**). With additional suction, the membrane patch underneath the pipette opening is ruptured (whole-cell configuration, **c**)

Experimental Protocol

The whole cell patch-clamp configuration is established by a sequence of pipette manoeuvres: At the beginning of the experimental procedure, a few disaggregated myocytes are placed in extracellular solution within a recording chamber mounted on an inverted microscope. By use of a micromanipulator, the patch pipette is positioned above a myocyte in the bath solution. At first the pipette filled with intracellular solution is lowered into the recording chamber. Slight positive pressure is applied to the pipette holder to prevent clotting of the pipette tip. At this stage, the amplifier indicates the pipette resistance and the offset of the amplifier has to be calibrated to 0 mV, which requires the calculation of the junction potential between intracellular and extracellular solution. While the pipette is placed next to a potential cell for recordings, the patch-clamp amplifier is set to voltage-clamp mode and the computer generates a rectangular pulse of about 5 mV. The patch pipette is placed on the cell membrane (see Fig. 11a) and gentle suction is applied to the pipette holder by an external vacuum syringe to facilitate the formation of a high-resistance seal between pipette tip and cell membrane (Giga-ohm seal, Fig. 11b). After giga-seal formation, further suction is applied (break-in) to rupture the membrane patch underneath the patch pipette and establish a whole-cell configuration for current recordings. The break in manoeuvre removes the barrier between intracellular medium and intracellular solution in the pipette. At this stage, changes in the holding potential will result in net ion fluxes across the entire cell membrane that can be recorded as whole cell currents.

The pulse protocol used for stimulation of the calcium channels under study depends on the aim of the experiment and the cells used. As stated before, different cell types differ in their electrophysiological properties, e.g. their resting membrane potential (Fig. 12).

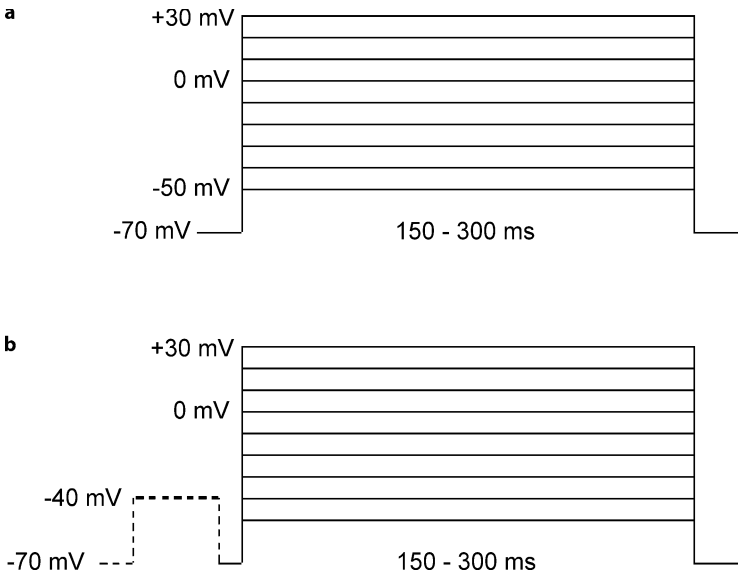

Figure 12a,b
Typical pulse protocol for whole-cell calcium current recordings. From a holding potential of –70 to –50 mV, depending on the cell type studied, depolarization steps to +30 mV in 10 mV increments are administered. If the Na^+ current is not blocked by pharmacological means (**a**), a depolarizing prepulse to –40 mV must be added to the protocol (**b**)

Single Channel Recording

In this approach to patch clamp recording, a small heat-polished glass pipette is pressed against the cell membrane forming an electrical seal. The method was first introduced by Neher and Sakmann. They electrically isolated small patches of membrane on frog muscle fibres by enzymatically cleaning them and then pressing the small glass pipette against them.

It was observed that tight pipette-membrane seals, with resistances of 10–100 GΩ, can be obtained when suction is applied to the pipette interior ("Giga-seal"). Giga-seals are mechanically very stable, so that if the pipette is withdrawn, the seal usually remains intact and the membrane patch is excised from the cell (Hamill et al. 1981). The high resistance, in parallel with the greatly reduced capacitance of a membrane patch having an area of only a few square micrometers, allows resolution of the microscopic ionic currents (pA-range, depending on test- and holding-potentials) that intermittently flow through any channels that happen to have been trapped in the membrane patch.

The high resistance of a "giga-seal" reduces the background noise of the recordings by an order of magnitude, and allows a patch of membrane to be voltage-clamped without the use of microelectrodes. Here are some helpful rules to produce a giga-seal. Avoid dirt on the pipette, using a fresh pipette for each seal. Each pipette should be used only after positive pressure has been relieved. Following enzyme treatment of muscle preparations, the surface of the bathing solution is frequently covered with debris with readily adheres to the pipette tip, preventing giga-seal formation. HEPES-

buffered pipette solutions should be used when calcium is present in the pipette solution. Filtered solutions should be used in the bath as well in the pipette. When a slight negative pressure of 20–30 cm H_2O was applied the resistance increased within a few seconds to ~20–80 GΩ. In some cases giga-seals develop spontaneously without suction. In other cases suction has to be applied for periods of 10–60 s, or a seal may develop only after suction has been released.

Recording Solutions

When a pipette is sealed tightly on to a cell it separates the total cell surface membrane into two parts: the area covered by the pipette (the patch area) and the rest of the cell. Solutions used to fill the pipette or to bathe cells will dependent on the currents and the type of cells to be studied. The solution mimics the normal and extracellular environments of mammalian cells. A typical patch pipette (usually borosilicate glass) is filled with pipette solution (first "tip filling" and then "back filling" with 110 mM $BaCl_2$, 10 mM HEPES, pH 7.4 – adjusted with tetraethylammonium hydroxide) and sealed against the surface membrane. Single channel experiments were performed in an external bath solution containing 120 mM K^+-glutamate, 25 mM KCl, 2 mM $MgCl_2$, 10 mM HEPES, 2 mM EGTA, 1 mM $CaCl_2$, 1 mM Na-ATP, and 10 mM dextrose, pH 7.4.

Pipette Fabrication

Borosilicate pipettes are pulled in two stages using a vertical microelectrode puller and the standard heating coils supplied with it. The capillary is thinned over a length of ~10 mm to obtain a minimum diameter of 200 μm. The glass is then recentred with respect to the heating coil and in the second pull the thinned part breaks, producing two pipettes. In order to reduce the pipette-bath capacitance and to form a hydrophobic surface, pipette shanks are coated with Sylgard to within 50 μm of the tip. Polishing of the glass wall at the pipette tip is done on a microforge shortly after Sylgard coating. We use pipettes with resistance values in the range 67 MΩ. These have openings diameters between 0.5 and 1 μm.

Recording calcium channels in the cell-attached configuration, the pulse protocol can be changed in different electrophysiological experiments (activation experiments, different depolarizing test pulses –10 to +30 mV and constant holding potentials –90 mV (Fig. 13), inactivation experiments, constant depolarizing test pulses and different holding potentials). Ba^{2+} currents were elicited by depolarization test pulses delivered at 0.5 Hz, recorded at 10 kHz and filtered at 2 kHz (–3 dB, four-pole Bessel) using an Axopatch 1 D or Axopatch 200 A (Axon Instruments).

Data-Analysis

Linear leak and capacity currents were digitally subtracted using the average currents of non-active sweeps (Fig. 14).

Openings and closures were identified using the half-criterion (pClamp 6.0). Data were further analyzed by histogram analysis (open-time and closed-time histograms). Closed time analysis was restricted to patches where only one channel was present. NP_o (the product of the number of channels in the patch times their individual open

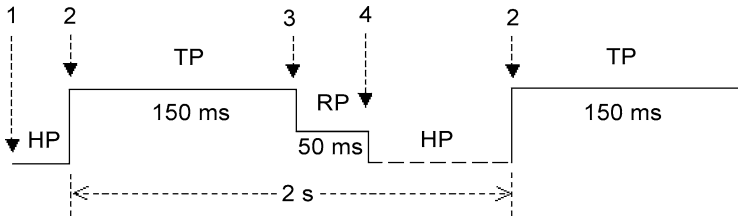

Figure 13
Typical pulse protocol for Ca^{2+} single-channel recording: *1* beginning of rest potential, *2* beginning of depolarization step, *3* end of depolarization step and beginning of repolarization, *4* end of repolarization, *HP* holding potential, *TP* test potential, *RP* repolarization potential, duration of all repetitive pulses 2 s (0.5 Hz), duration of depolarization 150 ms

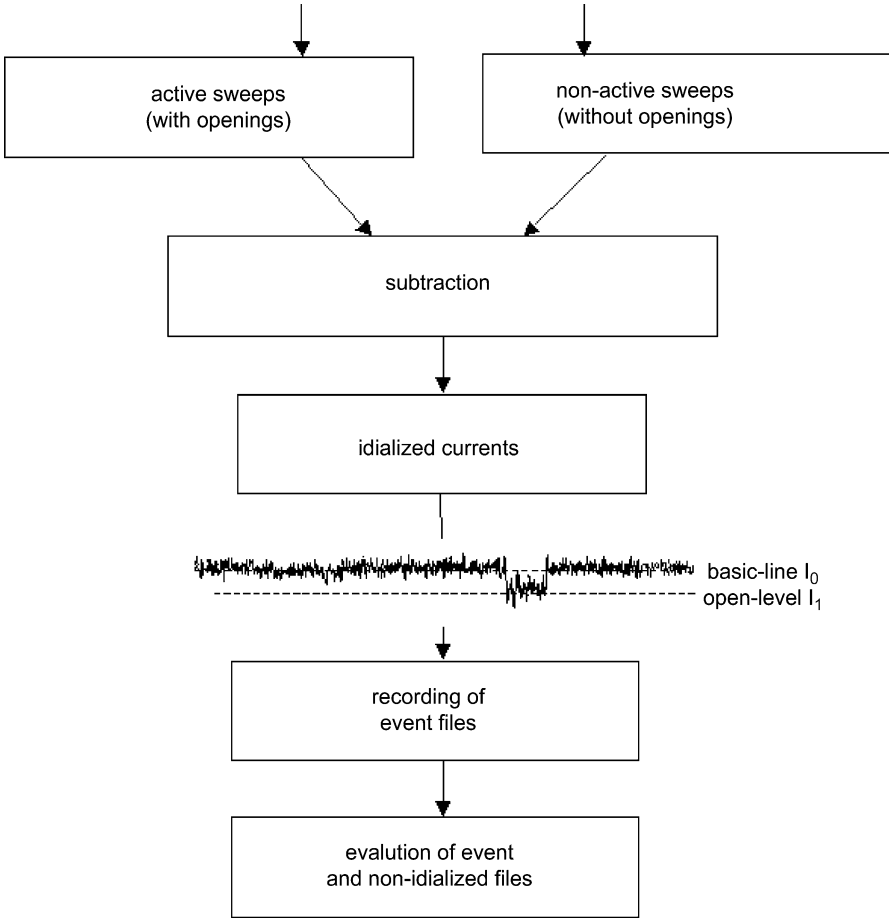

Figure 14
Algorithm of data analysis for single channel recordings

probability) was calculated as the ratio between total open time and the total recording time at the test potential. P_o (the single channel probability) was calculated as the ratio of the total open time and the total time recorded at the test potential, divided by the number of channels in the patch (N) where necessary and possible.

Activation and inactivation data were fitted to a Boltzmann-type function according to the following equation: $y = y_{max}\ 1/(1\ \exp\ [(V_{0.5} - V)/k])$, where y ($y_{max}$) is the (maximum) availability of channels, V is the membrane potential, $V_{0.5}$ is the potential at which activation or inactivation is half-maximal, and k is the slope factor describing the steepness of the curve at $V_{0.5.}$ (for detailed data-analysis, see Michels et al. 2002).

Examples

Basic Current Properties

A typical whole-cell L-type Ca^{2+} channel recording from guinea pig ventricular myocytes is shown in Fig. 15. Similar test potentials were applied in single-channel measurements of L-type Ca^{2+} channels in guinea ventricular myocytes demonstrated in Fig. 16.

Inactivation Kinetics in the Presence of Different Charge Carriers

According to reversal potential measurements estimated under bi-ionic conditions, the relative permeability sequence for divalent cations is $Ca^{2+} > Sr^{2+} > Ba^{2+}$, and $Li^+ > Na^+ > K^+ > Cs^+$ for monovalent cations. Under normal conditions monovalent cations are much less permeant than divalent ions. In the absence of external calcium however, calcium channels become highly permeable to monovalent ions. Hagiwara et al. (1974) concluded that this effect was caused by the fact that both ions compete for a common binding site at the channel pore, which has a weaker affinity for sodium. Figures 4 and 5 show Ba^{2+}, Sr^{2+} and Na^+ current measurements through the L-type Ca^{2+} channel in the absence of extracellular Ca^{2+}.

Obviously, in the presence of extracellular Ca^{2+} ions, at least one calcium ion is bound within the channel at all times, excluding monovalent ions from entering the channel pore (Hille 2001). Other divalent cations, such as Zn^{2+}, Co^{2+}, and Ni^{2+}, competing for the same binding site block L-type Ca^{2+} channels at concentrations of 10 μM to 20 μM.

Figure 4 shows the effect of different charge carriers (Ba^{2+}, Sr^{2+} and Na^+) on L-type Ca^{2+} current amplitude and current inactivation kinetics compared to recordings with Ca^{2+}. It is obvious that (1) in the absence of extracellular Ca^{2+} the channel becomes permeant for the cations studied, (2) increasing levels of depolarization accelerate current inactivation, and (3) that, as with all depolarization steps, inactivation is markedly slowed in the absence of extracellular Ca^{2+}. The last finding can be explained by an absence of calcium-dependent inactivation of the Ca^{2+} channel.

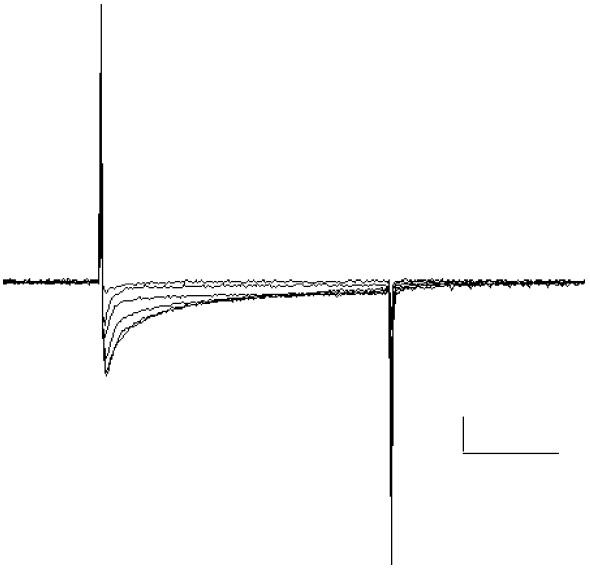

Figure 15
Typical L-type Ca^{2+} whole cell current elicited by step depolarizations of 300 ms duration from 30 mV to 20 mV. The current was recorded in guinea pig ventricular myocytes. The scale bars indicate 50 ms (horizontally) and 2.5 nA

Voltage-Dependent Inactivation

As discussed before, Ca^{2+} current inactivation is also affected by voltage. Findlay et al. (2002, see Fig. 5) showed that with increasing holding potentials from -20 to +20 mV, a step depolarisation to a fixed pulse potential resulted in faster inactivation kinetics. This was demonstrated with recordings where Ca^{2+} was replaced by Ba^{2+} (A and D), Sr^{2+} (B and E) and Na^{+} (C and F, see Fig. 5).

This characteristic is markedly reduced in the presence of 100 nM isoproterenol (D, E, F). As a result of β-adrenergic stimulation by isoproterenol, inactivation kinetics are slowed, due to a conversion of channels from a rapidly inactivating to a slowly inactivating kinetic form. With increasing holding potentials from –20to +20 mV, a step depolarisation to a fixed pulse potential results in faster inactivation kinetics. This effect is consistent between measurements with Ba^{2+}, Sr^{2+} and Na^{+} as charge carrier and does not therefore seem to be influenced by the charge carrier.

Modulation by DHP Ca^{2+} Agonists and Antagonists

Dihydropyridines comprise the two classes of agonistic and antagonistic Ca^{2+} channel modulators. Grabner et al. (1996) tested dihydropyridine sensitivity in chimeric Ca^{2+} channels generated with DHP-sensitive motifs transferred from L-type to originally DHP-insensitive brain calcium channels (see Fig. 9). In the presence of 10 μM BayK 8644, the total current amplitude was markedly increased, as opposed to recordings with isradipine.

Michels et al. (2002, see Fig. 10) showed similar results from single-channel measurements of single L-type Ca^{2+} channels in the presence of 0.1 mM BayK 8644. Due to the DHP Ca^{2+}-agonist, the single channel amplitude was increased from

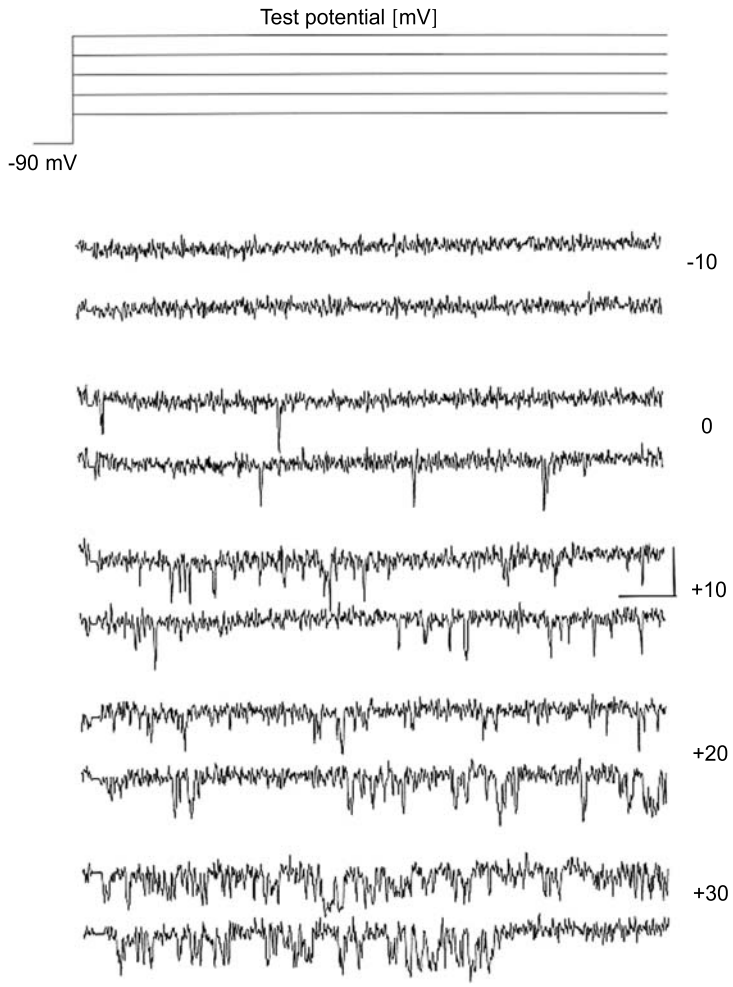

Figure 16
Single channel registration of L-type Ca^{2+} channel current at different test potentials (TP). The scale angle indicates 1 pA (*vertical*) and 15 ms (*horizontal*)

0.89 ± 0.04 pA to 1.13±0.09 pA and the average open-times were prolonged consistently.

Modulation by β-Adrenergic Activation

Under β-adrenergic stimulation, an increase in the Ca^{2+} current can be observed with further reduction of current inactivation. On a single-channel level, Schröder and Herzig (1999, see Fig. 6) showed an increase in channel availability with a larger number of openings and a markedly increased ensemble average current in the presence of 0.1 mM isoproterenol.

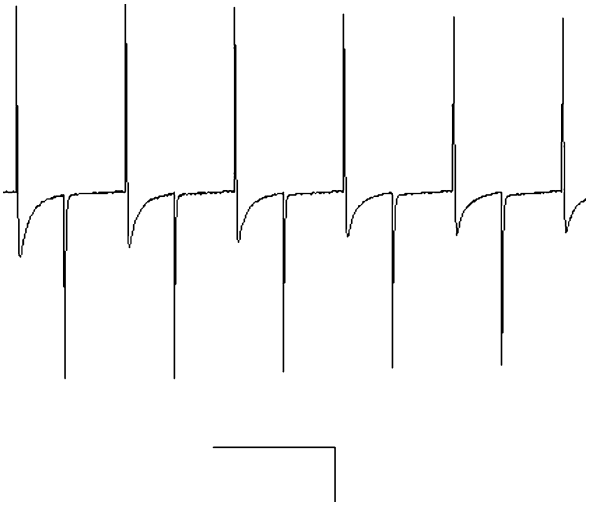

Figure 17
Ca^{2+} channel run-down elicited by repetitive depolarization to +10 mV in non-failing human ventricular cardiomyocytes at a frequency of 1 Hz. With an increasing number of stimulations, the current amplitude decreases steadily. The scale bars indicate 1000 ms (*horizontally*) and 0.1 nA (*vertically*)

Troubleshooting

Run-Down

Early investigators had already noticed that Ca^{2+} currents in various cell types tended to inactivate during long recordings under certain conditions, a phenomenon known as "run-down". Especially in whole cell recordings, dialysis of the intracellular medium by the intracellular solution in the tip of the patch pipette resulted in a steady decline in the current amplitude (Kostyuk et al. 1981). Similar results were seen in excised patch recordings where the membrane patch was immersed in an artificial intracellular solution (Nilius et al. 1985). This observation was independent of the charge carrier used, when extracellular Ca^{2+} was replaced by Ba^{2+}, run-down was not affected. Markwardt and Nilius (1990) showed that not only the total current amplitude but also current inactivation time constants decreased during calcium channel run-down in guinea-pig ventricular myocytes. From the work of a number of authors, various factors influencing the time-course of run-down have been identified. In the presence of Ca^{2+}-chelating agents (EDTA), Mg^{2+}ATP, cAMP and phosphodiesterase inhibitors, run-down could be prevented or even reversed. The same effect was observed when the catalytic subunit of protein kinase A (PKA) was added to the extracellular medium, indicating that Ca^{2+}-dependent phosphorylation and dephosphorylation of the Ca^{2+} channel are involved in run-down. Hao et al. (1999) separated the intracellular cytoplasmic extract into different fractions by gel filtration and found that a combination of an intracellular protein of >300 kD, called calpastatin and ATP restored the initial current amplitude by 87%. An example of Ca^{2+} whole cell current run-down by repetitive stimulation at a frequency of 1 Hz is demonstrated in Fig. 17.

Apart from adding Mg^{2+}ATP and EDTA to the pipette solution, run-down can be prevented by minimizing dialysis of the intracellular medium making use of the perforated patch method.

References

Adachi-Akanane S, Nagao T (2000) Ca^{2+} channel antagonists and agonists. In: Endo M, Kurachi Y, Mishina M. Pharmacology of ionic channel function. Activators and inhibitors. Springer, Berlin Heidelberg New York Tokyo

Bangalore R, Mehrke G, Gingrich D, Hofmann F, Kass RS (1996) Influence of L-type Ca channel alpha 2/delta-subunit on ionic and gating current in transiently transfected HEK 293 cells. Am J Physiol 270:H1521–H1528

Bean BP (1989) Neurotransmitter inhibition of neuronal calcium currents by changes in channel voltage-dependence. Nature 340: 153–155

Biel M, Ruth P, Bosse E, Hullin R, Stühmer W, Flockerzi V, Hofmann F (1990) Primary culture and functional expression of a high voltage activated calcium channel from rabbit lung. FEBS Letters 269: 409–412

Bodi I, Koch SE, Yamaguchi H, Szigeti GP, Schwartz A, Varadi G (2002) The role of region IVS5 of the human cardiac calcium channel in establishing inactivated channel conformation. J Biol Chem 277: 20651–20659

Diochot S, Richard S, Baldy-Moulinier M, Nargeot J, Valmier J (1995) Dihydropyridines, phenylalkylamines and benzothiazepines block N-, P/Q- and R-type calcium currents. Pflügers Arch 431: 10–19

Eberst R, Dai S, Klugbauer N, Hofmann F (1997) Identification and functional characterization of a calcium channel γ subunit. Pflügers Arch 433: 633–637

Ertel EA, Campbell KP, Harpold MM, Hofmann F, Mori Y, Perez-Reyes E, Schwartz A, Snutch TP, Tanabe T, Birnbaumer L, Tsien RW, Catterall WA (2000) Nomenclature of voltage-gated calcium channels. Neuron 25: 533–535

Findlay I (2002) Voltage- and cation-dependent inactivation of L-type Ca^{2+} currents in guinea-pig ventricular myocytes. J Physiol 541: 731–740

Fischmeister R, Hartzell HC (1986) Mechanism of action of acetylcholine on calcium currents in single cells from frog ventricle. J Physiol (Lond) 376: 183–202

Glossmann H, Ferry D, Striessnig J, Goll A, Moosburger K (1987) Resolving the structure of the Ca^{2+} channel by photoaffinity labelling. Trends Pharmacol Sci 8: 95–100

Glossmann H, Linn T, Rombusch M, Ferry DR (1983) Temperature-dependent regulation of d-cis[3H]diltiazem binding to Ca^{2+} channels by 1,4-dihydropyridine channel agonists and antagonists. FEBS Letters 160: 226–232

Grabner M, Wang Z, Hering S, Striessnig J, Glossmann H (1996) Transfer of 1,4-Dihydropyridine sensitivity from L-type to class-A (BI) calcium channels. Neuron 16: 207–218

Gurnett CA, DeWaard M, Campbell KP (1996) Dual function of the voltage-dependent Ca2+ channel alpha(2)delta subunit in current stimulation and subunit interaction. Neuron 1996; 16: 431–440

Hagiwara M, Adachi-Akahane S, Nagao T (1997) High-affinity binding of DTZ323, a novel derivate of diltiazem, to rabbit skeletal muscle L-type Ca^{2+} channels. J Pharmacol Exp Ther 281: 173–179

Hao L-Y, Kameyama A, Kameyama M (1999) A cytoplasmic factor, calpastatin and ATP together reverse run-down of Ca^{2+} channel activity in guinea-pig heart. J Physiol 514: 687–699

Hille B (2001) Ion channels of excitable membranes. Third Edition. Sinauer

Hirano Y, Yoshinaga T, Murata M, Hiraoka M (1999) Prepulse-induced mode 2 gating behaviour with and without β-adrenergic stimulation in cardiac L-type calcium channels. Am J Physiol 276: C1338–1345

Hoffmann F, Lacinová L, Klugbauer N (1999) Voltage-dependent calcium channels: From structure to function. Rev Physiol Biochem Pharmacol 139: 33–87

Kanaya S, Arlock P, Katzung BG, Hondeghem LM (1983) Diltiazem and verapamil preferentially block inactivated cardiac calcium channels. J Mol Cell Cardiol 15: 145–148

Klein G, Drexler H, Schröder F (2000) Protein kinase G reverses all isoproterenol induced changes of cardiac single L-type calcium channel gating. Cardiovasc Res 48: 367–374

Klugbauer N, Lacinová L, Marais E, Hobom M, Hofmann F (1999) Molecular diversity of the calcium channel $\alpha_2\delta$-subunit. J Neurosci 19: 684–691

Klugbauer N, Dai S, Specht V, Lacinova L, Marais E, Bohn G, Hofmann F (2000) A family of γ-like calcium channel subunits. FEBS Lett 470: 189–197

Kokubun S, Reuter H (1984) Dihydropyridine derivates prolong the open state of Ca channels in cultured cardiac cells. Proc Natl Acad Sci USA (Cell Biology) 81: 4824–4827

Kostyuk PG, Veselovsky NS, Fedulova SA (1981) Ionic currents in the somatic membrane of rat dorsal root ganglion neurons. II. Calcium currents. Neuroscience 7: 2431–2437

Kuo CC, Hess P (1993) Characterization of the high-affinity Ca^{2+} binding sites in the L-type Ca^{2+} channel pore in rat phaechromocytoma cells. J Physiol London 466: 657–682

Lee A, Wong ST, Gallagher D, Li B, Storm DR, Scheuer T, Catterall WA (1999) Ca^{2+}/calmodulin binds to and modulates P/Q-type calcium channel. Nature 399: 155–159

Lipkind GM, Fozzard HA (2003) Molecular modeling of interactions of dihydropyridines and phenylalkylamines with the inner pore of the L-type Ca^{2+} channel. Mol Pharmacol 63: 499–511

Markwardt F, Nilius B (1990) Changes of calcium channel inactivation during run-down. J Gen Physiol 9: 209–218

McDonald TF, Pelzer D, Trautwein W (1984) Cat ventricular muscle treated with D600: characteristics of calcium channel block and unblock. J Physiol 353: 217–241

Michels G, Matthes J, Handrock R, Kuchinke U, Groner F, Cribbs LL, Pereverzev A, Schneider T, Perez-Reyes E, Herzig S (2002) Single-channel pharmacology of mibefradil in human native T-type and recombinant $Ca_v3.2$ calcium channels. Mol Pharmacol 61: 682–694

Melzer W, Herrmann-Frank A, Lüttgau H C (1995) The role of Ca2+ ions in excitation-contraction coupling of skeletal muscle fibres. Biochimica et Biophysica Acta 1241: 59–116

Mitterdorfer J, Sinnegger MJ, Grabner M, Striessnig J, Glossmann H (1995) Coordination of Ca^{2+} by the pore region glutamates is essential for high-affinity dihydropyridine binding to the cardiac Ca^{2+} channel alpha 1 subunit. Biochmistry 34: 9350–9355

Mitterdorfer J, Wang Z, Sinnegger MJ, Hering S, Striessnig J, Grabner M, Glossmann H (1996) Two amino acid residues in the IIIS5 segment of L-type Ca^{2+} channels differentially contribute to 1,4-Dihydropyridine sensitivity. J Biol Chem 271: 30330–30335

Mitterdorfer J, Grabner M, Kraus RL, Hering S, Prinz H, Glossmann H, Striessnig J (1998) Molecular basis of drug interaction with L-type Ca2+ channels. J Bioenerg Biomembr 30: 319–334

Peterson BZ, Catterall WA (1995) Calcium binding in the pore of L-type calcium channels modulates high affinity dihydropyridine binding. J Biol Chem 270: 18201–18204

Peterson BZ, DeMaria CD, Adelman JP, Yue DT (1999) Calmodulin is the Ca^{2+} sensor for Ca^{2+} dependent inactivation of L-type calcium channels. Neuron 22: 549–558

Peterson BZ, Johnson BD, Hockerman GH, Acheson M, Scheuer T, Catterall WA (1997) Analysis of the dihydropyridine receptor site of L-type calcium channels by alanine scanning mutagenesis. J Biol Chem 272: 18752–18758

Quin N, Olcese R, Stefani E, Birnbaumer L (1998) Modulation of human neuronal $a_{1\,E}$-type calcium channel by $\alpha_2\delta$-subunit. Am J Physiol 274: C1324–C1331

Sanguinetti MC, Kass RS (1984) Voltage-dependent block of calcium channel current in calf cardiac Purkinje fiber by dihydropyridine calcium channel antagonists. Circ Res 55: 336–348

Sanguinetti MC, Krafte DS, Kass RS (1986) Voltage-dependent modulation of Ca channel current in heart cells by Bay K8644. J Gen Physiol 88: 369–392

Schramm M, ThomasG, Towart R, Franckowiak G (1983) Novel dihydropyridines with positive inotropic action through activation of Ca^{2+} channels. Nature 303: 535–537

Schröder F, Herzig S (1999) Effects of β_2-adrenergic stimulation on single-channel gating of rat cardiac L-type Ca^{2+} channels. Am J Physiol 276:H834–H843

Soldatov NM, Zühlke RD, Bouron A, Reuter H (1997) Molecular Structures Involved in L-type Calcium Channel Inactivation. Role of the carboxyl-terminal region encoded by exons 40–42 in a1C subunit in the kinetics and Ca^{2+} dependence of inactivation. J Biol Chem 272: 3560–3566

Triggle DJ (1996). The classification of calcium antagonists. J Cardiovasc Pharmacol. 27 (Suppl A):S11–S16

Viard P, Exner T, Maier U, Mironneau J, Nurnberg B, Macrez N (1999) Gbγ dimers stimulate vascular L-type Ca^{2+} channels via phosphoinositide 3-kinase. FASEB J 13: 685–694

Walker D, De Waard M (1998) Subunit interaction sites in voltage-dependent Ca^{2+} channels: role in channel function. Trends Neurosi 21: 148–154

Yamaguchi H, Muth J, Varadi M, Schwartz A, Varadi G (1999) Critical role of conserved proline residues in the transmembrane segment 4 voltage sensor function and in the gating of L-type calcium channels. PNAS 96: 1357–1362

Yue DJ, Backx PH, Imredy JP (1990a) Calcium sensitive inactivation in the gating single calcium channel. Science 250: 1735–1738

Yue DJ, Marban E (1990b) Permeation in the dihydropyridine-sensitivity calcium channel: multiple occupany but no anomalous mole-fraction effect between Ba^{2+} and Ca^{2+}. J Gen Physiol 95: 911–939

Zhang JF, Ellinor PT, Aldrich RW, Tsien RW (1994) Molecular determinants of voltage dependent inactivation in calcium channels. Nature 327: 97–100